

Groundwater Research Report  
WR01R010

**MONITORING AND SCALING OF WATER  
QUALITY IN THE TOMORROW-  
WAUPACA WATERSHED**

**Bryant A. Browne  
Nathan M. Guldán**

Funding Year: 2001

# **Monitoring and Scaling of Water Quality in the Tomorrow-Waupaca Watershed**

Bryant A. Browne, Associate Professor of Soil and Water Resources  
Nathan M. Guldan, Graduate Student  
College of Natural Resources  
University of Wisconsin-Stevens Point

## TABLE OF CONTENTS

LIST OF FIGURES	3
PROJECT SUMMARY	4
INTRODUCTION	6
STUDY AREA	7
PROCEDURES AND METHODS	7
RESULTS AND DISCUSSION	8
CONCLUSIONS AND RECOMMENDATIONS	14
REFERENCES	15
APPENDIX A	17
APPENDIX B	18

## LIST OF FIGURES

Figure 1.	Annual N-fertilizer sales in Wisconsin and the U.S. 1960 - 1995.	6
Figure 2.	Location of the Tomorrow/Waupaca River Watershed in central Wisconsin with the location of sampling sites and stream order indicated.	7
Figure 3.	a) Relationship between measured $\text{NO}_3^-$ , N-fertilizer sales, and apparent recharge date, b) Relationship between $\text{XsN}_2$ and apparent recharge date, c) Relationship between Total $\text{NO}_3^-$ and apparent recharge date.	10
Figure 4.	a) Lag time distribution for discharging groundwater samples assuming a normal distribution with a mean of 28 years and a standard deviation of $\pm 12$ years. Normal distribution curves represent baseflow sampling dates of 2002, 2022, and 2042. b) Possible lag time distributions of tributary streams (A, B, C) and the composite of the 3 tributaries (D, dashed line). The color scheme represents a hypothetical pattern of average total $\text{NO}_3^-$ concentrations in annual groundwater recharge. The inset is a schematic of the hypothetical stream system, showing baseflow sampling positions and a minipiezometer network.	11
Figure 5.	a) Relationship between denitrification efficiency and apparent recharge date. b) Relationship between denitrification efficiency and $\text{O}_2$ .	12
Figure 6.	Relationship between estimated recharge total $\text{NO}_3^-$ and recharge date and between estimated specific discharge weighted total $\text{NO}_3^-$ , total $\text{NO}_3^-$ assuming an electron ( $e^-$ ) donor limitation, and total $\text{NO}_3^-$ assuming an $\text{NO}_3^-$ limitation and sample date. Annual and October mean $\text{NO}_3^-$ concentrations measured in TWR baseflow in 1975, 1995, and 2002 are shown as solid circles.	13

# **Monitoring and Scaling of Water Quality in the Tomorrow-Waupaca Watershed**

R/UW-SAM-002

by

Bryant A. Browne, Associate Professor of Soil and Water Resources

Nathan M. Guldán, Graduate Student

College of Natural Resources, University of Wisconsin-Stevens Point

**Contract:** July 1, 2001 – June 30, 2003

**Funding:** University of Wisconsin System (UWS)

**Focus Area:** SAM

**Key Words:** Denitrification, Nitrate, Groundwater Age, CFCs, Spatial Scale, Temporal Scale, Baseflow Water Quality

## **Background/Need**

Nitrate ( $\text{NO}_3^-$ ) concentrations in groundwater fed streams are frequently lower than concentrations in groundwater beneath adjacent agricultural recharge areas. The cause of this discrepancy and similar discrepancies for other chemicals poses a key question for understanding how agricultural practices affect water quality in many river systems. Unfortunately, conventional stream monitoring approaches are insufficient to address this question.

Two factors that contribute to differences in groundwater  $\text{NO}_3^-$  concentrations between recharge areas and stream discharge points are: 1) the transformation of  $\text{NO}_3^-$  to gaseous forms (nitrous oxide, nitrogen gas) by denitrifying bacteria and 2) the amount of time it takes groundwater to move through the landscape from recharge areas to discharge points (lag time). To predict how these factors affect baseflow water quality a better understanding of the spatial and temporal scales of groundwater/surface water interactions is needed.

## **Objectives**

The objectives of this study were to characterize the spatial and temporal scales of groundwater discharge to a 4<sup>th</sup> order stream within an agricultural basin and to quantify the influence of groundwater denitrification on baseflow  $\text{NO}_3^-$  concentrations.

## **Methods**

This study was conducted in the Tomorrow/Waupaca River Watershed which is located in parts of Portage, Waupaca, and Waushara Counties in central Wisconsin. A network of miniature wells (minipiezometers) along 1<sup>st</sup> through 4<sup>th</sup> order stream corridors was established to map the primary discharge areas. The well screens were installed at a depth of approximately 70 cm below the streambed in order to sample groundwater immediately before it discharged to the stream. Groundwater samples were collected from the minipiezometers in late summer and fall 2002 to map the chemical characteristics of discharge to the stream network. Surface water samples were collected on October 19, 2002 to create a corresponding map of the baseflow water quality. Groundwater gas samples were collected from each minipiezometer in late summer and fall 2002 to determine the amount of denitrification occurring and to determine the lag time of the groundwater using chlorofluorocarbons (CFCs).

## Results and Discussion

Baseflow was primarily derived from zones of discharge within 1<sup>st</sup> and 2<sup>nd</sup> order drainage corridors. Discharge occurred at a spatial scale of < 50,000 m cumulative stream length. Beyond 50,000 m cumulative stream length there was little communication between groundwater and surface water.

Contemporary baseflow was comprised, on average, of groundwater recharged nearly three decades ago, and reflected a temporal scale spanning nearly a half century. The mean lag time of groundwater discharge measured by apparent CFC age-dating was 28 ( $\pm$  12) yrs.

Contemporary baseflow NO<sub>3</sub><sup>-</sup> concentrations were strongly affected by denitrification in groundwater. The concentration of denitrified N was more or less constant across the 50-yr temporal scale. Denitrification reaction progress (percent of groundwater NO<sub>3</sub><sup>-</sup> converted to harmless N<sub>2</sub> gas) was nearly complete (86%) in older groundwater (> 32 yr), which contributes about one-third of the discharge to the TWR, due to low O<sub>2</sub> and the availability of e<sup>-</sup> donors. But reaction progress declined dramatically in younger groundwater (< 32 yr) in association with rising NO<sub>3</sub><sup>-</sup> concentrations, higher O<sub>2</sub>, and limited availability of e<sup>-</sup> donors. Overall, more than half (59%) of the NO<sub>3</sub><sup>-</sup> carried in groundwater was transformed to harmless N<sub>2</sub> gas by denitrifying bacteria before its release to baseflow.

Current concentrations of total NO<sub>3</sub><sup>-</sup> (NO<sub>3</sub><sup>-</sup> + denitrified N) in discharge to the TWR reflected land use practices between 1950 and the early 1990s, and strongly parallel the historical rise of N-fertilizer use. Using lag time distribution and denitrification data, stream baseflow NO<sub>3</sub><sup>-</sup> concentrations were projected over a 110-yr period centered on the present (2002). Predicted baseflow NO<sub>3</sub><sup>-</sup> concentrations were consistent with available historical baseflow data (1975, 1995, 2002). Projections for the future under a stable land use scenario suggest that rising baseflow NO<sub>3</sub><sup>-</sup> concentrations will plateau between 2005 and 2020.

## Conclusions/Implications/Recommendations

The lag time between groundwater recharge and groundwater discharge to baseflow dominated streams has confounded attempts to use conventional baseflow water quality monitoring approaches to assess relationships between land use practices and water quality in river systems.

In this study, we show that a basin-scale synoptic survey (combining water quality and recharge age-date measurements) at the groundwater/surface water interface is a highly effective tool for deciphering relationships between historic land use and contemporary and future baseflow water quality.

Similar lag time/denitrification studies should be performed in other basins where a longer baseflow water quality record will allow a more rigorous validation of baseflow projections against historical data.

## Related Publications

None at this time.

## INTRODUCTION

Stream water quality is substantially determined by the quality of groundwater discharge in baseflow dominated stream systems. However, during baseflow periods, stream nitrate ( $\text{NO}_3^-$ ) concentrations tend to be lower than groundwater  $\text{NO}_3^-$  concentrations in adjacent agricultural recharge areas (Bohlke and Denver, 1995; Bohlke et al., 2002; Molénat et al., 2002; Puckett et al., 2002). Two factors that contribute to differences in groundwater  $\text{NO}_3^-$  concentrations between recharge areas and discharge points are: 1) the transformation of  $\text{NO}_3^-$  to gaseous forms (nitrous oxide, nitrogen gas) by denitrifying bacteria and 2) the amount of time it takes groundwater to move through the landscape from recharge areas to discharge points (lag time).

Denitrification may occur anywhere along the flowpath where there is a sufficient concentration of labile electron ( $e^-$ ) donors (e.g. dissolved organic carbon, reduced manganese, ferrous iron, sulfides) and anoxic or  $\text{O}_2$  depleted conditions to reduce  $\text{NO}_3^-$  to  $\text{N}_2$  or  $\text{N}_2\text{O}$  (Korom, 1992). Active locations within groundwater flow systems potentially include the water table/capillary fringe environment (Haag and Kaupenjohann, 2001), along the flowpath (particularly where groundwater encounters patches of organic debris; Puckett and Cowdery, 2002), within the riparian subsurface (Sabater et al., 2003), or within the hyporheic zone (Duff and Triska, 1990). Groundwater discharge affected by denitrification will be depleted of  $\text{NO}_3^-$  to some degree and enriched with excess  $\text{N}_2$  ( $\text{XsN}_2$ ) above atmospheric  $\text{N}_2$  levels (Korom, 1992).

Lag time contributes to differences between groundwater and baseflow  $\text{NO}_3^-$  concentrations due to changes in land use over time. For example, due to the increased N-fertilizer use over the last several decades (Fig. 1), discharging groundwater with lag times greater than 40 years would be expected to have little or no  $\text{NO}_3^-$  from agriculture, while groundwater with lag times less than 40 years would be expected to contain varying amounts of  $\text{NO}_3^-$  with the concentration dependent on the year recharge occurred. Together, denitrification and lag time confound attempts to relate baseflow stream  $\text{NO}_3^-$  concentrations to current and historical land use.

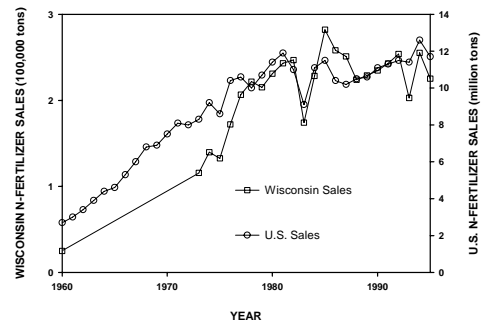


Figure 1 Annual N-fertilizer sales in Wisconsin and the U.S. 1960 – 1995 (USDA, 1997).

Although several studies have addressed the effect of lag time (Katz et al., 2001), denitrification (Puckett and Cowdery, 2002), or both (Bohlke and Denver, 1995; Bohlke et al., 2002) on groundwater  $\text{NO}_3^-$  concentrations, they have focused mainly on changes along groundwater flowpaths or at a few groundwater discharge areas of a watershed. There have been no attempts to quantify the combined influence of lag time and denitrification at the scale of a small basin. In this study we use a basin-scale network of wells to capture groundwater immediately before it discharges to the Tomorrow/Waupaca River (TWR), a fourth order, baseflow dominated stream in an agriculturally dominated landscape in central Wisconsin. We develop a basin-wide estimate of groundwater denitrification efficiency (percent of  $\text{NO}_3^-$  converted to  $\text{XsN}_2$  gas through denitrification) for the watershed, quantify the lag times of the discharging groundwater using dissolved chlorofluorocarbons (CFCs) as recharge age-dating tools (Busenberg and

Plummer, 1992), and examine the combined influence of denitrification and lag time on current stream water quality.

## STUDY AREA

The Tomorrow/Waupaca River Watershed (TWRW) is located in parts of Portage, Waupaca, and Waushara Counties in central Wisconsin (Fig. 2). The TWR is a tributary of the Wolf River within the Lake Michigan Drainage Basin. The watershed encompasses 790 km<sup>2</sup> and contains approximately 80 lakes and 362 km of stream. The estimated drainage density of the watershed is 0.47 km/km<sup>2</sup>. Baseflow accounts for 80 to 90% of the annual stream flow in the watershed while direct runoff accounts for 10 to 20% of the stream flow.

The watershed is dominated by agricultural land use. Sixty-one percent of the watershed is currently used for agriculture (Weister, 1995), which reportedly represents a decline of approximately 25% since 1948 (Bradley, 2003). Of the current agricultural land, most (82%) is nonirrigated and used to produce field corn and hay; the remainder (18%) is irrigated and used to produce potatoes, peas, sweet corn, snap beans, soybeans, and cucumbers. In 1998 there were approximately 145 dairy operations in the watershed (Cook, 2000). The watershed includes 32% forested land, 3% wetlands, and 2% water. About 2% of the landscape is urban; the watershed has approximately 13,000 residents (Weister, 1995; Bradley and Rahmeier, 1995).

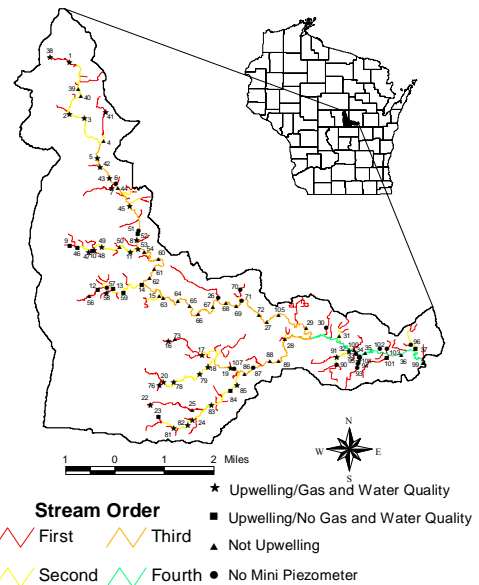


Figure 2 Location of the Tomorrow/Waupaca River Watershed in central Wisconsin with the location of sampling sites and stream order indicated.

## PROCEDURES and METHODS

We established a network of miniature wells (minipiezometers) along 1<sup>st</sup> through 4<sup>th</sup> order stream corridors to map the primary discharge areas (Fig. 2). The minipiezometers were constructed of polyethylene tubing (i.d. 6.8 mm) with 2.54 cm well screens. The screens were placed at a depth (dz) of approximately 70 cm below the streambed in order to sample groundwater immediately before it discharged to the stream. Water level (dh) within the minipiezometers was measured relative to the stream surface. The primary areas of discharge were identified by the distribution of positive dh values within the drainage network during the late summer and fall of 2002. Hydraulic conductivity was measured by the falling head test (Hvorslev, 1951). Specific discharge (q) was calculated using the following Darcy's Law relationship:

$$q = -K \cdot (dh/dz) \quad [1]$$

Groundwater samples were collected from the minipiezometers to map the chemical characteristics (dissolved solids and dissolved gases) of discharge to the stream network. Surface water samples were collected on October 19, 2002 to create a corresponding map of the baseflow water quality (dissolved solids only). Stream flow was measured using the dye dilution method (Rantz, 1982).



Groundwater gas samples were harvested from minipiezometers using pumping induced ebullition (PIE, Browne, 2003). Gas chromatography procedures (Browne, 2003) were used to measure dissolved concentrations of Ar, N<sub>2</sub>, O<sub>2</sub>, N<sub>2</sub>O, CO<sub>2</sub>, CH<sub>4</sub>, CFC-11, CFC-12, and CFC-113. The concentration of denitrified N (XsN<sub>2</sub>) in groundwater discharge was determined from the concentration of dissolved N<sub>2</sub> gas in excess of atmospheric equilibrium (Heaton and Vogel, 1981; Busenberg et al., 1993).

$$XsN_2 = \text{Total } N_2 - \text{Atmospheric } N_2 \quad [2]$$

(Argon was used as an atmospheric reference gas to determine the concentration of N<sub>2</sub> derived from the atmosphere.) The total concentration of NO<sub>3</sub><sup>-</sup> was reconstructed by summing the measured NO<sub>3</sub><sup>-</sup> and XsN<sub>2</sub> concentrations:

$$\text{Total } NO_3^- = NO_3^- + 2 \cdot XsN_2 \quad [3]$$

Lag time estimates were calculated from apparent groundwater recharge dates based on the mole fractions of atmospheric chlorofluorocarbons (CFCs) within PIE gas samples. Due to solubility of gases within atmospheric moisture, CFCs have accumulated at ultra-trace levels within the hydrosphere in conjunction with their accumulation in the atmosphere. Because their rapid atmospheric accumulation has been well-documented from about 1940 to the present and because detection at ultra-trace levels (about one part per trillion in gas) is possible using common laboratory instrumentation (GC ECD), CFCs have become valuable tracers for groundwater recharge age-dating (Busenberg and Plummer, 1992; 2000; Puckett et al., 2002). The premise of CFC age-dating is that the volume or mole fraction of CFCs within the gases dissolved in groundwater reflects the atmospheric volume fraction (mixing ratio) of CFCs during the year of groundwater recharge. In this study, the volume fractions of CFC-11, CFC-12 and CFC-113 measured within the PIE gas samples, adjusted to the temperature of groundwater recharge using Henry's Law relationships, were compared to historic records of CFC atmospheric mixing ratios to determine the year of groundwater recharge (the "apparent CFC recharge age-date"). Lag time was then calculated by subtracting the apparent recharge date from the year of sample collection:

$$\text{Lag Time} = 2002 - \text{Apparent CFC Recharge Date} \quad [4]$$

## RESULTS and DISCUSSION

### Spatial Scale of Groundwater Discharge within the Tomorrow/Waupaca River Watershed

Forty-seven minipiezometers had static head (dh) levels above the stream water surface indicative of a gaining stream segment. Significantly, 89% of the gaining locations were concentrated in low order ( $\leq 3$ ) streams at positions upstream of 50,000 m cumulative stream length. Nongaining minipiezometer locations ( $n = 32$ ) were mostly (69%) concentrated beyond 50,000 m cumulative stream length. These results suggested that baseflow water quality beyond 50,000 m cumulative stream length was largely determined by upstream discharge to low order stream channels. Consistent with this idea, we found that the mean dissolved solids concentrations within groundwater discharge were generally not significantly different ( $\alpha < 0.05$ ) from baseflow water quality beyond 50,000 m cumulative stream length. Thus, beyond the 50,000 m cumulative stream length position, baseflow concentrations of conservative chemical constituents were essentially a physical average (a composite by mixing) of the basin-wide quality of groundwater discharge.

### **Influence of Groundwater Denitrification on Baseflow $\text{NO}_3^-$**

The dissolved concentration of  $\text{XsN}_2$  ranged from below detection (14  $\mu\text{mol/L}$ ) up to 186  $\mu\text{mol/L}$ , representing a conversion of up to 373  $\mu\text{mol/L}$  of  $\text{NO}_3^-$  to  $\text{N}_2$  gas in groundwater by denitrifying bacteria. The basin-wide mean concentration of  $\text{XsN}_2$  in groundwater discharge, weighted by specific discharge, was 71  $\mu\text{mol/L}$ , corresponding to a basin-wide mean concentration of denitrified N of 141  $\mu\text{mol/L}$ .

Estimates of the total  $\text{NO}_3^-$  concentration (Appendix B) in the discharging groundwater were reconstructed by summing the concentrations of  $\text{NO}_3^-$  and  $\text{XsN}_2$  gas (Eq. [3]). For many locations the concentration of total  $\text{NO}_3^-$  was substantially higher than the concentration of  $\text{NO}_3^-$ . Total  $\text{NO}_3^-$  ranged from 137 - 1245  $\mu\text{mol/L}$ , while  $\text{NO}_3^-$  alone ranged from 7 - 1171  $\mu\text{mol/L}$ . The overall specific discharge weighted mean concentration of total  $\text{NO}_3^-$  ( $362 \pm 266$   $\mu\text{mol/L}$ ) in groundwater discharge was nearly double the specific discharge weighted mean concentration of  $\text{NO}_3^-$  ( $218 \pm 297$   $\mu\text{mol/L}$ ). The efficiency (or progress) of groundwater denitrification (Eq. [5]), defined as the ratio of denitrified N to total  $\text{NO}_3^-$  (Bohlke et al., 2002)

$$\% \xi = \frac{2 \bullet \text{XsN}_2}{\text{NO}_3^- + 2 \bullet \text{XsN}_2} \bullet 100 \quad [5]$$

ranged from 0% to 98%, with a median value of approximately 71% (Appendix B). The basin-wide efficiency of denitrification estimated by the specific discharge weighted mean was 59% ( $\pm 36\%$ ), indicating that more than half of the groundwater  $\text{NO}_3^-$  load was reduced to harmless  $\text{N}_2$  gas prior to discharge to the TWR.

### **Temporal Scale of Baseflow $\text{NO}_3^-$ - Influence of Lag Time**

The apparent CFC recharge dates of groundwater discharge to the TWR ranged from 1953 to 2002 (Appendix B), with a specific discharge weighted mean of 1974 ( $\pm 12$  yr). Corresponding apparent lag times (Eq. [4]) ranged from 0 to 49 yrs, indicating that the discharging groundwater represents a temporal scale of nearly a half century. The basin-wide mean apparent lag time weighted by specific discharge was 28 ( $\pm 12$ ) yr.

Figure 3a illustrates  $\text{NO}_3^-$  concentrations in groundwater discharge in relation to apparent CFC recharge dates. The rising concentrations of  $\text{NO}_3^-$  can mainly be attributed to the import of fixed N into the agricultural areas of the Tomorrow/Waupaca River Basin (TWRB) rather than a change in land cover percent (agricultural land use has declined by approximately 25% in the TWRB since 1948; Bradley, 2003). However, the pattern of  $\text{NO}_3^-$  contamination is difficult to reconcile with the historical rise of agricultural N use because the rise in contamination is offset from fertilizer N sales by 10 to 15 years. Concentrations were near zero in groundwater recharged prior to 1970, then rose steeply in groundwater recharged after 1970 and approached (excluding a mid-1970s outlier) 600  $\mu\text{mol/L}$  on the upper end in groundwater recharged in the late 1980s. In contrast, the sale of agricultural N in Wisconsin and the U.S. (Fig. 1) rose steadily from the late 1950s through the late 1980s.

Reconstruction of total  $\text{NO}_3^-$  concentrations (Eq. [3]) eliminated the apparent delay in the onset of contamination, revealing a stronger relationship with agricultural N over the last 40 years (Fig. 3c). Regression of total  $\text{NO}_3^-$  versus apparent recharge date revealed that 18% of the variance ( $r^2$

= 0.18) of the groundwater  $\text{NO}_3^-$  concentration was explained by the apparent recharge date. The slope of the regression line suggests that the average  $\text{NO}_3^-$  concentration in annual groundwater recharge of the TWRB has increased by  $6.25 (\pm 2.44) \mu\text{mol L}^{-1} \text{yr}^{-1}$  since the mid-1950s. Based on the average slope of the fertilizer sales data for Wisconsin ( $10,830 \text{ tons yr}^{-1}$ ) and the U.S. ( $438,300 \text{ tons yr}^{-1}$ ) from 1960 - 1981, the groundwater quality response to N-fertilizer is approximately  $0.00058 \mu\text{mol L}^{-1} \text{ton}^{-1}$  (WI) and  $0.000014 \mu\text{mol L}^{-1} \text{ton}^{-1}$  (U.S.).

The regression line in Figure 3c can be conceived as a representation of the spatially averaged annual mean total  $\text{NO}_3^-$  concentration in TWRB groundwater recharge over four decades. The variance unexplained by the regression model can be attributed to spatial variation in land use within groundwater recharge areas of the TWRB. Variation around the annual mean widened appreciably from the mid-1950s through the 1990s as N use increased within the landscape. The lower extremes of the annual distributions remained fairly constant in time and arguably represent groundwater recharged within non-agricultural areas of the basin. The upper extremes of the annual distributions, which represent groundwater recharged within agricultural areas, are predominantly responsible for the rising mean annual  $\text{NO}_3^-$  concentrations represented by the regression line. Thus, a combination of temporal and spatial variation of groundwater recharge, captured in Figure 3c, is responsible for the average quality of groundwater currently discharging to the TWR.

Ignoring for the moment the influence of denitrification (addressed below), two considerations are important in attempting to interpret current  $\text{NO}_3^-$  concentrations in TWR baseflow in context of these observations. The first consideration is that lag time is not a specific value but a distribution of values, which represent a moving window of time. The moments of the age distribution (e.g., mean, standard deviation, skewness) determine when and how intensely the groundwater quality signal of a particular recharge year will be expressed in the stream baseflow. The second consideration is that the lag time distribution of groundwater contributing to the contemporary baseflow of a stream reflects a specific spatial scale.

In Figure 4a the TWRB lag time distribution (simplified as a hypothetical normal distribution with a mean = 28 yrs and a standard deviation of  $\pm 12$  yrs) is shifted along the time axis to illustrate relative proportions of groundwater contributing discharge on three baseflow sampling dates (2002, 2022, and 2042). These distributions are further superimposed upon a hypothetical

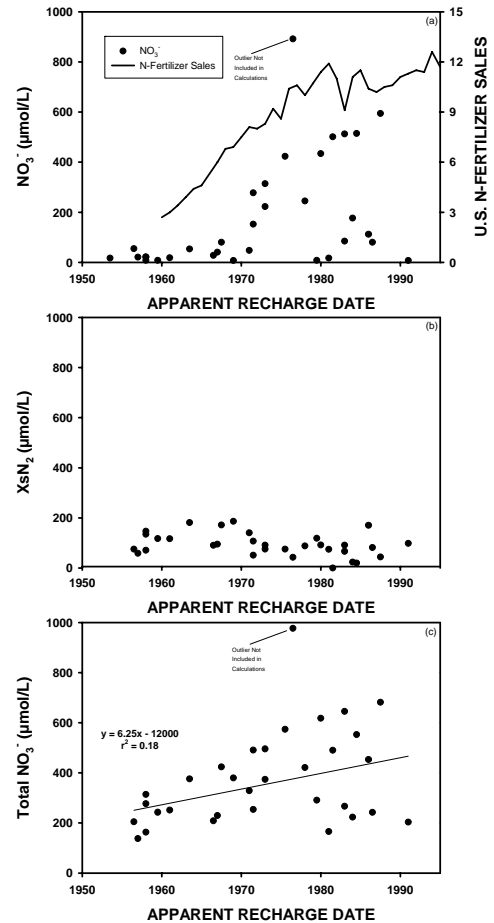


Figure 3 a) Relationship between measured  $\text{NO}_3^-$ , N-fertilizer sales, and apparent recharge date, b) Relationship between  $\text{XsN}_2$  and apparent recharge date, c) Relationship between Total  $\text{NO}_3^-$  and apparent recharge date.

color representation of the spatially averaged mean annual concentrations of total  $\text{NO}_3^-$  in groundwater recharge to illustrate the composition of groundwater contributing to baseflow. The mean lag time of 28 yrs determines that baseflow  $\text{NO}_3^-$  concentrations observed in 2002, 2022 and 2042 are mostly determined by the composition of groundwater recharged in 1974, 1994 and 2014 (the mean recharge dates), respectively, but the variance of the age distribution dampens the signal of the mean recharge date by physically blending it (i.e. mixing the colors in Fig. 4a) with older and younger water. Thus, with respect to contemporary baseflow in the TWR, these observations suggest that the  $\text{NO}_3^-$  concentration beyond 50,000 m cumulative stream length is most strongly influenced by the spatially averaged concentration in groundwater recharged around 1974 but the signal of 1974 groundwater is diluted by groundwater recharged in the mid-1950s through the early 1990s.

To illustrate the importance of sampling scale, in Figure 4b we show lag time distributions for three hypothetical 1<sup>st</sup> order tributaries (ABC) to a 2<sup>nd</sup> order stream system (D, inset Fig. 4b). Basin A has the largest average lag time with a moderately narrow lag time distribution ( $40 \pm 5$  yrs), and it accounts for 30% of baseflow in tributary D. Basin B has an intermediate average lag time with a fairly broad lag time distribution ( $28 \pm 8$  yrs), and it accounts for 50% of flow in tributary D. And Basin C has the smallest average lag time and the narrowest lag time distribution ( $15 \pm 3$  yrs), and it accounts for 20% of flow in tributary D. Contemporary (e.g., 2003) baseflow water quality from the outlet of tributary A would most intensely reflect groundwater recharged in the early 1960s. Baseflow water quality in tributary B would have a signal of groundwater recharged in 1975 relatively well blended with 1960s and 1980s groundwater recharge. At tributary C, baseflow water quality would carry the relative strong signal of late 1980s groundwater recharge weakly dilute by early 1980s and early 1990s groundwater recharge. At the scale of the 2<sup>nd</sup> order tributary D (Fig. 4b) the combined lag time distribution obtained by summing the distribution and weighting for discharge, would appear as distribution D (dashed line). Hence, the baseflow water quality in tributary D would have a fairly uniform distribution of recharge water quality covering a 40-yr period from 1950 through 2000. Accordingly, the TWRB lag time distribution data obtained from the minipiezometer network are relevant at a cumulative stream length of 50,000 m, a scale which encompasses basin-wide groundwater discharge. Thus, the application of this age-distribution at the scale of one of the TWR's individual 1<sup>st</sup> or 2<sup>nd</sup> order sub-

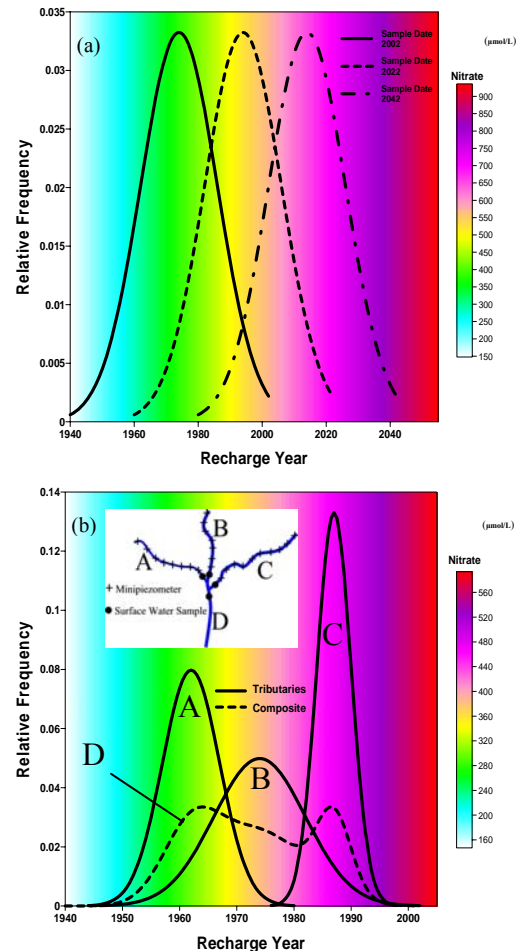


Figure 4 a) Lag time distribution for discharging groundwater samples assuming a normal distribution with a mean of 28 years and a standard deviation of  $\pm 12$  years. Normal distribution curves represent baseflow sampling dates of 2002, 2022, and 2042. b) Possible lag time distributions of tributary streams (A, B, C) and the composite of the 3 tributaries (D, dashed line). The color scheme represents a hypothetical pattern of average total  $\text{NO}_3^-$  concentrations in annual groundwater recharge. The inset is a schematic of the hypothetical stream system, showing baseflow sampling positions and a minipiezometer network.

basins would be inappropriate.

### Lag Time and Denitrification Efficiency

The concentration of  $XsN_2$  gas remained more or less constant across the entire timescale (Fig. 3b). Thus, the denitrification efficiency (Fig. 5a) shows a strong downward trend with apparent recharge date in the post-1970 data as total  $NO_3^-$  concentrations rise. Although  $O_2$  appears to be an important factor controlling this decline (Fig. 5b), different mechanisms are likely important in pre-1970 (apparent age > 32 yrs) and post-1970 (apparent age < 32 yrs) groundwater discharge.

At discharge locations where apparent age exceeded 32 years, nearly all  $NO_3^-$  was converted to  $XsN_2$  under low dissolved  $O_2$  levels (the mean  $O_2$  concentration was  $45 \pm 24 \mu\text{mol/L}$ ). The mean denitrification efficiency weighted by specific discharge was 86% ( $\pm 7\%$ ). Largely uninhibited by  $O_2$ , it is unclear whether denitrification capacity (availability of  $e^-$  donors) or availability of  $NO_3^-$  controlled the formation of  $XsN_2$  in these discharge waters. Thus, whether denitrification capacity in > 32-yr-old discharge waters, which potentially account for a third or more of the discharge to the TWR, will eventually be overwhelmed by the rising  $NO_3^-$  loads in groundwater is an important question for understanding future baseflow water quality.

At discharge locations where apparent age was < 32 years, conditions were markedly different. Here, rising  $NO_3^-$  concentrations, accompanied by widely varying  $O_2$  concentrations ( $206 \pm 95 \mu\text{mol/L}$ ), appear to have overwhelmed the denitrification capacity in groundwater. The mean denitrification efficiency weighted by specific discharge was 47% ( $\pm 36\%$ ) in these discharge waters. Absent a  $NO_3^-$  limitation, denitrification efficiency dropped steeply in post-1970 groundwater discharge wherever total  $NO_3^-$  concentrations exceeded pre-1970 levels. Inhibition by  $O_2$  probably explains most of decreased denitrification efficiency (Fig. 5b), but lack of availability of  $e^-$  donors (e.g., DOC) cannot be ruled out as a contributing factor. Thus, discharge from locations with apparent ages < 32 years, which potentially account for nearly two-thirds of groundwater discharge to the TWR, could potentially drive a long-term rise in baseflow  $NO_3^-$  concentrations in TWR.

### Backcasted and Forecasted $NO_3^-$ Concentrations in Baseflow

Figure 6 illustrates the importance of both lag time and denitrification for understanding contemporary baseflow  $NO_3^-$  concentrations and other water quality conditions in the TWR beyond 50,000 m cumulative stream length.

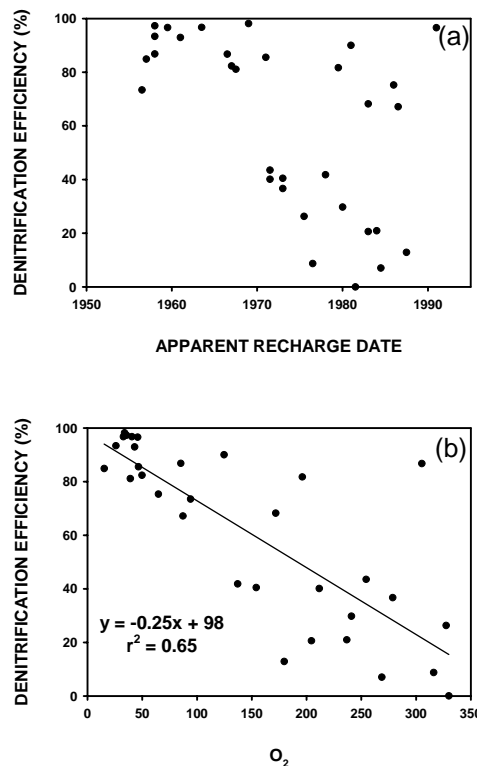
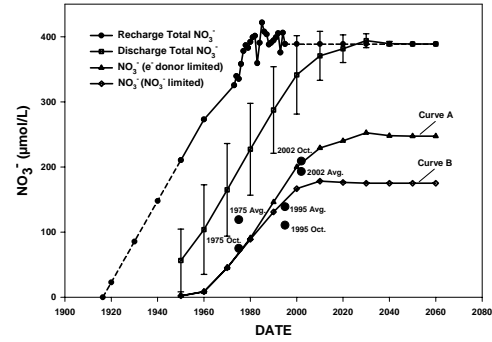


Figure 5 a) Relationship between denitrification efficiency and apparent recharge date. b) Relationship between denitrification efficiency and  $O_2$ .

Figure 6 Relationship between estimated recharge total  $\text{NO}_3^-$  and recharge date and between estimated specific discharge weighted total  $\text{NO}_3^-$ , total  $\text{NO}_3^-$  assuming an electron ( $e^-$ ) donor limitation, and total  $\text{NO}_3^-$  assuming an  $\text{NO}_3^-$  limitation and sample date. Annual and October mean  $\text{NO}_3^-$  concentrations measured in TWR baseflow in 1975, 1995, and 2002 are shown as solid circles.

Estimates of the annual mean total  $\text{NO}_3^-$  concentration in groundwater recharge were projected over a 110 year period centered on the present. The section of curve that predates the fertilizer sales records (pre-1960) was generated by extrapolating the regression in Figure 3c backward from 1960 through 1916. Estimates for the period between 1960 and 1995 were based on the total  $\text{NO}_3^-$ /Wisconsin N-fertilizer sales response ( $0.00058 \mu\text{mol L}^{-1} \text{ton}^{-1}$ ) discussed above and annual N-fertilizer sales illustrated in Figure 1. (For example, between 1973 and 1974, N-fertilizer sales increased by 24,050 tons, potentially increasing the total  $\text{NO}_3^-$  concentration by  $14 \mu\text{mol L}^{-1}$  ( $0.00058 \mu\text{mol L}^{-1} \text{ton}^{-1}$ ) from  $325 \mu\text{mol L}^{-1}$  in 1973 to  $339 \mu\text{mol L}^{-1}$  in 1974.) For the post-1995 estimates, the fertilizer N sales were assumed to stabilize at their 1995 value. In order to generate estimates of total  $\text{NO}_3^-$  concentrations in groundwater discharge, the total  $\text{NO}_3^-$  recharge estimates were subsampled using the specific discharge weighted age distribution of the year 2002 dataset (See conceptual approach in Figure 4a.). Subsamples were generated at 10-yr intervals by shifting the age-distribution along the time axis. The calculated means and standard deviations of total  $\text{NO}_3^-$  concentrations in groundwater discharge depict the hypothetical progression of baseflow water quality composition at decadal intervals in the TWR if no groundwater denitrification occurred.



Comparison of the rising portions of the total  $\text{NO}_3^-$  curves (recharge and discharge) in Figure 6, which reflect the period of sharply increasing agricultural N use, show that the expression of recharge water quality within baseflow is delayed by nearly three decades due to the lag time between the upland recharge areas and the stream discharge positions. The flattened, overlapping portions of the two curves, which reflect the plateau in agricultural N use, reveal that total  $\text{NO}_3^-$  can approach a steady state in groundwater (recharge = discharge = baseflow) of the TWR if land management practices remain relatively constant for periods longer than 30 years. These observations underscore the idea that attempts to correlate current baseflow water quality monitoring data to current land use practices (e.g., fertilizer use) using conventional streamflow monitoring approaches will yield little useful information in basins like the TWRB.

The total  $\text{NO}_3^-$  concentrations in groundwater discharge were adjusted in two ways for groundwater denitrification in order to generate corresponding estimates of  $\text{NO}_3^-$  in baseflow of the TWR (Fig. 6). In the first approach (curve A), denitrification was assumed to be  $e^-$  donor limited,  $\text{O}_2$  limited or both in all TWRB groundwater. Under this assumption, the specific discharge weighted mean denitrified N for the 2000 dataset ( $141 \mu\text{mol/L}$ ) was taken as a basin-wide estimate of the denitrification capacity of groundwater and was subtracted from all total  $\text{NO}_3^-$  values within a subsample (outcomes with negative  $\text{NO}_3^-$  concentrations were assigned a value of zero). In the second approach (curve B), denitrification was assumed to be  $\text{NO}_3^-$  limited in groundwater with ages  $> 32$  yrs but again assumed to be  $e^-$  donor or  $\text{O}_2$  limited in groundwater with ages  $< 32$  yrs. Thus, concentrations of  $\text{NO}_3^-$  were assigned a value of zero in groundwater with ages  $> 32$  yrs under the assumption that  $X_{\text{SN}_2} = \text{total } \text{NO}_3^-$ , and concentrations of  $\text{NO}_3^-$  in groundwater with ages  $< 32$  yrs were calculated as in the first approach.

The importance of denitrification for controlling the past and future concentration of  $\text{NO}_3^-$  in the TWR baseflow is revealed by comparing the groundwater discharge curves for total  $\text{NO}_3^-$  and  $\text{NO}_3^-$  in Figure 6. Until about 1960 the denitrification capacity of groundwater prevented entry of  $\text{NO}_3^-$  from agriculture and other land uses into the TWR. Thereafter, the curves suggest that N loadings within the landscape began to exceed the groundwater denitrification capacity, accounting for the eventual rise of  $\text{NO}_3^-$  concentrations in baseflow. Based on the assumption of a uniform denitrification capacity of  $141 \mu\text{mol/L}$  (curve A), the denitrification efficiency would have declined from nearly 100% in pre-1960 baseflow to approximately 41% by 2000; and would be projected to remain at 41% if total  $\text{NO}_3^-$  concentrations remain steady in groundwater recharge. Under the assumption that  $> 32$ -yr groundwater retains near 100% denitrification efficiency (curve B), the denitrified N in groundwater discharge approaches  $214 \mu\text{mol/L}$ , and provide approximately 55% denitrification efficiency beyond 2000. Because discharge of  $> 32$ -yr groundwater may provide a third of the baseflow in the TWR, a better understanding of the factors controlling denitrification capacity in older groundwater is important for predicting future water quality.

Available information on the historical concentration of  $\text{NO}_3^-$  in baseflow of the TWR is limited to 1975, 1995, and 2002. In Figure 6 we compare measured annual and October means for  $\text{NO}_3^-$  in TWR baseflow to the predicted  $\text{NO}_3^-$  concentration in baseflow ( $\text{NO}_3^-$  discharge curves A and B). The measured baseflow  $\text{NO}_3^-$  concentrations are consistent with the  $\text{NO}_3^-$  projections based on both lag time and denitrification.

Projections in Figure 6 suggest that rising baseflow  $\text{NO}_3^-$  concentrations will plateau between 2005 and 2020 under a stable land use scenario. Similar lag time/denitrification studies should be performed in other basins where a longer baseflow water quality record will allow a more rigorous verification of baseflow projections against historical data. These results suggest that basin-scale synoptic surveys (water quality and recharge age-date measurements) at the groundwater/surface water interface are highly effective tools for deciphering relationships between land use and future baseflow water quality.

## CONCLUSIONS and RECOMMENDATIONS

- We studied the influences of groundwater denitrification and lag time (residence time of groundwater between recharge and discharge) on contemporary  $\text{NO}_3^-$  concentrations in baseflow of a 4<sup>th</sup> order stream within an agricultural watershed. Using a network of minipiezometers we obtained a basin-scale sample of groundwater discharge immediately before its release to the stream.
- Discharge occurs at a spatial scale of  $< 50,000$  m cumulative stream length in the TWR. Beyond 50,000 m cumulative stream length there was little communication between groundwater and surface water. Baseflow was primarily derived from zones of discharge within 1<sup>st</sup> and 2<sup>nd</sup> order drainage corridors.
- Contemporary baseflow  $\text{NO}_3^-$  concentrations are strongly affected by denitrification in groundwater. More than half (59%) of the  $\text{NO}_3^-$  carried in groundwater was transformed to harmless  $\text{N}_2$  gas by denitrifying bacteria before its release to baseflow.

- Contemporary baseflow is comprised, on average, of groundwater recharged nearly three decades ago, reflecting a temporal scale of nearly 50 years. The mean lag time of groundwater discharge measured by apparent CFC age-dating was 28 ( $\pm$  12) yrs.
- Current concentrations of total  $\text{NO}_3^-$  ( $\text{NO}_3^-$  + denitrified N) in discharge to the stream encompass nearly 50 years of land use practices (between 1950 and the 1990s) and strongly reflect the historical rise of fertilizer N use.
- The concentration of denitrified N was more or less constant across the temporal scale. Denitrification reaction progress was nearly complete (86%) in older groundwater ( $>$  32 yr), which contributes about one-third of the discharge to the TWR, due to low  $\text{O}_2$  and the availability of  $e^-$  donors. But reaction progress declined dramatically in younger groundwater, which accounts for about two-thirds of groundwater discharge to the TWR, due to rising  $\text{NO}_3^-$  concentrations, higher  $\text{O}_2$ , and limited availability of  $e^-$  donors.
- Using lag time distribution and denitrification data, stream baseflow  $\text{NO}_3^-$  concentrations were projected over a 110-yr period centered on the present (2002). Predicted baseflow  $\text{NO}_3^-$  concentrations were consistent with available historical baseflow data (1975, 1995, 2002). Projections for the future under a stable land use scenario suggest that rising baseflow  $\text{NO}_3^-$  concentrations will plateau between 2005 and 2020.
- Our results suggest that basin-scale synoptic surveys (water quality and recharge age-date measurements) at the groundwater/surface water interface can be highly effective tools for deciphering relationships between historic land use and contemporary and future baseflow water quality. Similar lag time/denitrification studies should be performed in other basins where a longer baseflow water quality record will allow a more rigorous verification of baseflow projections against historical baseflow water quality data.

## REFERENCES

- Bohlke, J.K. and J.M. Denver. 1995. Combined use of groundwater dating, chemical, and isotopic analyses to resolve the history and fate of nitrate contamination in two agricultural watersheds, Atlantic coastal plain, Maryland. *Water Resources Research* 31:2319-2339.
- Bohlke, J.K., R. Wanty, M. Tuttle, G. Delin, and M. Landon. 2002. Denitrification in the recharge area and discharge area of a transient agricultural nitrate plume in a glacial outwash sand aquifer, Minnesota. *Water Resources Research* vol 38, no 7, [np]. Jul 2002.
- Bradley, S. 2003. Personal Communication. Portage County Planning and Zoning Department, Stevens Point, Wisconsin.
- Bradley, S., and K. Rahmeier. 1995. Nonpoint source control plan for the Tomorrow/Waupaca River priority watershed project. Wisconsin Department of Natural Resources. Publication WR-434-95, 119 p.
- Browne, B.A. 2003, Draft. Pumping induced ebullition: A unified and simplified method for measuring multiple dissolved gases. For submission to *Environmental Science and Technology*.
- Busenberg, E. and L.N. Plummer. 1992. Use of chlorofluorocarbons as hydrologic tracers and age-dating tools: The alluvium and terrace system of central Oklahoma. *Water Resources Research* 28:2257-2283.
- Busenberg, E., E.P. Weeks, L.N. Plummer, and R.C. Bartholomay. 1993. Age dating ground water by use of chlorofluorocarbons ( $\text{CCl}_3\text{F}$  and  $\text{CCl}_2\text{F}_2$ ), and distribution of



- chlorofluorocarbons in the unsaturated zone, Snake River Plain aquifer, Idaho National Engineering laboratory, Idaho. U.S. Geological Survey Water-Resources Investigations 93-4054, 47 p.
- Cook, R.C. 2000. Relationships between private well water, stream base flow water, and land use in the Tomorrow-Waupaca River Watershed. M.S. thesis. University of Wisconsin-Stevens Point, Stevens Point, WI.
- Duff, J.H. and F.J. Triska. 1990. Denitrification in sediments from the hyporheic zone adjacent to a small forested stream. *Canadian Journal of Fisheries and Aquatic Sciences* 47:1140-1147.
- Haag, D. and M. Kaupenjohann. 2001. Landscape fate of nitrate fluxes and emissions in Central Europe. A critical review of concepts, data, and models for transport and retention. *Agriculture, Ecosystems and Environment* 86:1-21.
- Heaton, T.H.E., and J.C. Vogel. 1981. "Excess air" in groundwater. *Journal of Hydrology* 50:201-216.
- Hvorslev, M.J. 1951. Time-lag and soil permeability in ground water observations. Bull. 36. U.S. Army Eng. Waterways Exp. Sta., Vicksburg, MS.
- Katz, B.G., J.K. Bohlke, and H.D. Hornsby. 2001. Timescales for nitrate contamination of spring waters, northern Florida, USA. *Chemical Geology* 179:167-186.
- Korom, S.F. 1992. Natural denitrification in the saturated zone: A review. *Water Resources Research* 28:1657-1668.
- Molénat, J., P. Durand, C. Gascuel-Oudou, P. Davy, and G. Gruau. 2002. Mechanisms of nitrate transfer from soil to stream in an agricultural watershed of French Brittany. *Water, Air, and Soil Pollution* 133:161-183.
- Puckett, L.J. and T.K. Cowdery. 2002. Transport and fate of nitrate in a glacial outwash aquifer in relation to ground water age, land use practices, and redox processes. *Journal of Environmental Quality* 31:782-796.
- Rantz, S.E. 1982. Measurement and computation of streamflow: Volume 1. Measurement of stage and discharge. U.S. Geological Survey Water-Supply Paper 2175, 284 p.
- Sabater, S., D. Dowrick, M. Hefting, V. Maitre, G. Pinay, C. Postolache, M. Rzepecki, F. Sabater, A. Butturini, J.-C. Clement, and T. Burt. 2003. Nitrogen removal by riparian buffers along a European climatic gradient: Patterns and factors of variation. *Ecosystems* 6:20-30.
- United States Department of Agriculture. 1997. Agricultural Resources and Environmental Indicators, 1996-1997. Agricultural Handbook No. 712. Economic Research Service, Natural Resources and Environmental Division. Washington, DC, 497 pp.
- Weister, C.L. 1995. Tomorrow/Waupaca River Priority Watershed Groundwater Resource Appraisal. Wisconsin Department of Natural Resources Final Report.

## **APPENDIX A**

None at this time.

## APPENDIX B

**Dissolved solids and specific discharge of groundwater samples.**

Site	Temp	pH	SPC	DOC	DIC	DRP	NO <sub>3</sub> <sup>-</sup>	Cl <sup>-</sup>	SO <sub>4</sub> <sup>-</sup>	NH <sub>4</sub> <sup>+</sup>	Na <sup>+</sup>	K <sup>+</sup>	Mg <sup>2+</sup>	Ca <sup>2+</sup>	Mn <sup>2+</sup>	Fe <sup>2+</sup>	Specific Discharge
	°C		µS/cm	µmol													cm/s
1	12.6	7.21	389	566.9	4251	1.0	21.6	57.8	93.7	9.9	121.7	25.1	827	818	†	†	0.0109
2	13.9	7.57	363	59.7	3413	0.3	176.6	137.2	203.1	0.0	104.3	21.8	831	713	†	†	0.0085
3	16.5	7.08	1106	981.6	5371	13.0	17.1	7507	46.2	67.5	1478	156.4	1333	1480	†	†	0.0041
5	12.4	7.41	408	99.9	4523	1.6	21.0	96.7	243.6	8.8	108.7	27.4	985	678	†	†	0.0039
7	14.8	7.22	426	75.7	4421	0.3	80.2	153.8	246.0	0.0	139.1	33.8	955	716	†	†	0.0020
8	13.4	7.60	482	50.4	2848	0.2	1170.	636.0	436.9	0.0	152.2	20.5	1006	895	†	†	0.0060
11	13.3	7.67	459	54.2	4059	0.0	514.2	123.0	109.5	0.0	213.0	26.2	1022	851	0.0	0.0	0.0078
16	10.1	7.77	153	38.1	2685	0.0	16.6	16.9	217.1	0.0	73.9	13.1	670	628	0.0	0.0	0.0401
17	14.7	7.59	368	83.8	3350	0.3	7.0	65.3	163.5	1.2	100.0	20.0	892	645	1.1	0.0	0.0027
18	11.3	7.65	264	33.1	4052	0.0	433.9	348.0	211.4	0.0	117.4	23.1	1061	912	0.0	0.0	0.0001
19	11.6	7.76	352	175.0	3811	0.3	7.6	112.1	2.7	17.9	187.0	41.3	819	736	1.5	3.9	0.0010
20	11.6	7.77	416	39.6	3924	0.0	152.3	43.5	163.4	0.0	100.0	20.5	945	790	0.0	0.0	0.0028
22	10.7	7.22	414	59.4	3735	0.2	245.1	85.1	163.8	0.0	95.7	18.7	907	787	0.0	0.0	0.0020
24	9.1	7.77	353	16.1	3579	0.0	54.4	22.8	105.6	0.0	121.7	34.9	840	698	0.0	0.0	0.0075
32	16.8	7.43	575	157.9	4277	0.3	112.3	848.9	684.8	0.0	739.1	43.6	1051	939	0.0	0.0	0.0006
38	13.0	7.76	325	148.7	2834	0.8	7.2	136.0	213.3	4.7	100.0	16.2	656	699	0.0	6.3	0.0026
41	12.5	7.43	303	793.8	5256	0.6	20.8	246.2	38.2	20.4	130.4	23.8	999	941	†	†	0.0198
42a	8.6	7.43	477	160.6	3496	0.6	500.9	247.2	230.1	0.0	152.2	23.3	946	796	†	†	0.0161
42b	6.9	7.82	425	28.0	2955	0.5	422.8	141.1	156.5	0.0	134.7	24.4	845	751	0.0	0.0	0.0004
43	14.3	7.79	396	23.9	4002	0.0	313.9	139.7	149.5	0.0	130.4	24.6	972	823	0.0	0.0	0.0011
45	13.2	7.52	432	99.7	4288	0.5	17.8	1433.	93.5	9.1	1043.	47.4	793	663	†	†	0.0018
47	11.8	7.84	472	78.4	5067	0.5	314.4	377.9	291.0	0.0	130.4	30.8	1160	725	†	†	0.0003
48	8.0	7.43	418	51.7	4104	0.1	40.6	23.6	138.9	0.0	100.0	47.7	994	831	0.0	0.0	0.0027
49	15.7	7.38	372	28.3	4098	0.4	27.8	37.5	183.0	0.0	165.2	51.5	897	677	†	†	0.0007
53	11.5	7.40	572	76.4	3984	0.0	594.0	534.4	253.3	0.0	434.8	69.2	1072	944	0.0	0.0	0.0006
58	9.2	7.57	†	81.5	4102	0.8	47.7	134.4	488.4	3.3	130.4	33.8	1005	794	†	†	0.0056
76	14.0	7.39	220	44.6	3424	0.0	84.7	41.7	236.2	0.0	104.3	22.8	854	728	0.0	0.0	0.0105
78	9.8	7.69	412	37.4	3506	0.3	277.4	131.6	196.0	0.0	117.4	22.8	952	791	0.0	0.0	0.0037
79	14.0	7.56	395	46.8	3366	0.7	222.6	88.0	195.6	0.0	117.4	30.2	918	742	0.0	0.0	0.0078
81	9.8	7.83	507	50.9	3448	0.0	891.9	322.3	328.2	0.7	160.9	14.4	1115	914	0.0	0.0	0.0111
82	11.4	7.49	382	68.8	4094	0.8	79.7	493.7	239.1	0.0	782.6	16.7	899	809	0.0	0.0	0.0007
83	9.9	8.16	362	33.3	3569	0.0	8.1	20.7	124.2	1.1	139.1	37.2	873	684	1.5	3.9	0.0009
85	7.7	8.11	200	82.2	2567	0.0	8.0	85.2	220.1	0.0	121.7	11.5	440	475	0.0	0.0	0.0023
91	12.1	7.57	477	190.3	1476	0.0	53.3	218.1	465.0	0.0	356.5	51.0	1065	874	3.3	8.6	0.0047
95	13.2	7.46	661	145.4	4862	0.2	512.6	1025.	380.6	0.0	391.3	25.4	1295	1080	0.0	0.0	0.0109

† No data available.

Concentration, mean ( $\mu$ ), standard deviation (SD), specific discharge weighted mean ( $\mu_w$ ), and weighted standard deviation ( $SD_w$ ) of dissolved gases, excess  $N_2$  ( $XsN_2$ ), denitrified  $NO_3^-$  ( $dNO_3^-$ ),  $NO_3^-$ , and total  $NO_3^-$ , denitrification efficiency ( $\% \xi$ ), and CFC recharge date of groundwater samples (RD).

Site	$O_2$	$CO_2$	$CH_4$	$N_2O$	Ar	$N_2$	$XsN_2$	$dNO_3^-$	$NO_3^-$	Total	$\% \xi$	RD
										$NO_3^-$		
$\mu\text{mol/L}$											%	yr
1	85	179	18.4	†	14.3	542	71	141	22	163	87	1958
2	237	209	0.00	0.12	18.8	636	23	46	177	223	21	1984
3	†	133	0.58	0.04	†	†	†	†	17	†	†	1953
5	26	344	0.54	0.00	19.0	749	146	293	21	314	93	1958
7	39	111	†	0.08	17.8	738	172	343	80	423	81	1967
8	340	28	†	0.07	17.0	596	37	74	1171	1245	6	2002
11	269	†	0.00	0.16	19.3	653	19	39	514	553	7	1984
16	125	†	0.00	0.00	19.5	729	74	149	17	166	90	1981
17	46	†	0.04	0.00	20.8	771	98	196	7	203	97	1991
18	241	187	0.06	0.67	20.8	774	92	183	434	618	30	1980
19	36	167	6.10	0.33	18.5	765	135	269	8	276	97	1958
20	212	†	0.00	0.00	20.3	713	51	101	152	254	40	1971
22	137	†	0.05	0.00	20.8	766	88	176	245	421	42	1978
24	94	†	0.02	0.00	20.8	761	75	150	54	204	73	1956
32	65	†	0.19	0.00	18.8	785	170	340	112	453	75	1986
38	34	†	3.51	0.00	19.5	828	186	373	7	380	98	1969
41	15	703	38.6	0.00	20.0	732	58	116	21	137	85	1957
42a	330	204	0.00	0.30	18.6	605	0	0	501	490	0	1981
42b	328	†	0.00	0.23	19.2	709	75	151	423	573	26	1975
43	279	178	2.08	0.37	22.3	821	91	181	314	495	37	1973
45	43	286	†	0.02	18.3	724	117	233	18	251	93	1961
47	318	†	0.00	0.00	19.0	645	15	31	314	345	9	2002
48	50	†	0.11	0.00	19.5	736	95	189	41	229	82	1967
49	305	80	†	0.00	16.5	642	90	181	28	208	87	1966
53	180	†	0.01	0.43	18.5	673	44	87	594	681	13	1987
58	47	†	2.56	0.00	18.3	748	140	280	48	328	85	1971
76	172	†	0.00	0.00	19.5	734	91	181	85	266	68	1983
78	254	21	0.03	0.03	21.0	794	107	213	277	490	43	1975
79	154	†	0.00	0.28	19.3	705	75	151	222	373	40	1973
81	316	†	0.02	0.21	20.0	694	43	85	892	977	9	1976
82	87	†	0.02	0.00	20.0	755	81	163	80	242	67	1986
83	41	†	2.26	0.00	20.8	812	117	234	8	243	97	1959
85	196	63	0.05	0.27	22.8	864	119	237	8	291	82	1979
91	33	396	1.65	0.00	19.5	832	181	363	53	376	97	1963
95	204	†	0.00	0.52	18.5	683	66	133	513	645	21	1983
$\mu$	157	206	2.5	0.12	19.3	727	89	179	214	398	58	1974
SD	111	169	7.5	0.18	1.6	73	48	96	274	235	34	13
$\mu_w$	157	303	5.2	0.10	19.1	702	71	141	218	362	59	1974
$SD_w$	104	234	12.0	0.15	1.5	69	41	82	297	266	36	12

† No data available